

## TRISTAN ACHIEVEMENTS AND FUTURE PLANS

Shigeru Isagawa

KEK

National Laboratory for High Energy Physics  
1-1 Oho, Tsukuba, Ibaraki-ken, 305, Japan

## ABSTRACT

TRISTAN has achieved the peak luminosity of  $1.4 \times 10^{31} \text{ cm}^{-2}\text{s}^{-1}$  at a new energy range of (28+28) GeV. Programs to upgrade beam energy and luminosity of TRISTAN are in progress. The beam energy is to be increased to 30 ~ 33 GeV by use of superconducting RF cavities by the end of 1989. An addition of superconducting quadrupole magnets to the present low beta insertion is expected to double the luminosity.

## I. INTRODUCTION

In November 1986, a new energy frontier has been opened up for elementary particle physics with the completion of the high energy  $e^+e^-$  colliding beam accelerator TRISTAN (Transposable Ring Intersecting Storage Accelerator in Nippon). On 19th of this month, exactly five years after the ground breaking ceremony, the first electron-positron collision event at 48 GeV, the world highest  $e^+e^-$  collision energy, was successfully observed by one of the major detectors, VENUS.<sup>1,3)</sup>

Since then other two general purpose apparatus called AMY and TOPAZ, and a rather small-scale special purpose detector, SHIP, moved into the beam collision areas. After some preliminary runs, the regular operation of the TRISTAN accelerator for the physics data taking was started in May 1987. In the course of the operations, the accelerator performance has been rapidly improved: the machine energy went up and the peak luminosity increased substantially.

In this report we will first outline the TRISTAN accelerator system and summarize its present status and performance. The future aspects of its upgrading will also be described.

## II. OUTLINE OF TRISTAN ACCELERATOR SYSTEM<sup>4,5)</sup>

A layout of the TRISTAN accelerator complex is illustrated in Fig. 1. One-dot-chain line shows the boundary of the KEK site. The complex consists of an injector linac system, an accumulation ring, AR, and a main colliding beam ring, MR. The injector system is composed of a 2.5 GeV main linac, a 200 MeV high current  $e^-$  linac which produces positrons, and a 250 MeV linac which preaccelerates positrons before injection into the main linac. The main linac, 400 m in length, has been operated since 1982. It can provide 2.5 GeV beams to AR in a short pulse mode (1 ns) and to the photon factory electron storage ring (PF) in a long pulse mode (0.2 ~ 1  $\mu$ s).

AR is a storage accelerator which accumulates and accelerates electrons and positrons up to 6.5 ~ 8 GeV before transferring them to MR. The principal parameters of AR and MR are given in Table 1. In MR, two electron and two positron bunches circulate clockwise and counter-clockwise, respectively, and collide with each other at the midpoint of the four straight sections, where the experimental detectors are set up. As shown in Fig. 1 they are installed in four large experimental halls, which are named as Tsukuba, Oho, Fuji and Nikko in clockwise direction.

Figure 2 is a layout of AR and the beam transport lines. In AR there are two RF halls (East and West) for RF acceleration, two experimental halls for beam collision experiments (North and South), and an additional experimental hall along the North-East arc for the synchrotron radiation research (SRR). The electron and positron beams are injected from the 2.5 GeV linac through the injection transport lines. The accumulated beams are accelerated in AR,

and transferred to MR via the crossed beam transport lines. All the beam ducts and the vacuum components are made of aluminum alloys. A special extrusion process and a new fabricating technique mostly developed by KEK made it possible to complete a very good ultra-high vacuum system.<sup>6)</sup> An example of the pressure distribution along the entire circumference of AR and MR during the collision experiments is shown in Fig. 3. The average pressure achieved is in the order of  $10^{-7}$  Pa. Each magnet in MR was aligned within an average error of  $\pm 0.2$  mm (rms) along the 3 km circumference.<sup>7)</sup> The beam orbit can be measured with an accuracy of  $\pm 0.05$  mm by use of 400 sets of position monitors made out of electrostatic pickup discs along the MR.<sup>8)</sup> The whole TRISTAN accelerator complex except for the linac is controlled from a single console in the central control room (CCR). Distributed computer system and their excellent man-machine interface capability make the operation of TRISTAN very convenient and handy.<sup>9,10)</sup>

### III. TRISTAN COMISSIONING AND OPERATION

TRISTAN was proposed at KEK as early as 1974. In April 1981 this project was approved by the Government of Japan. In October, 1981, a call for letters of intent for TRISTAN experiments was issued. And on the day, November 19, 1981, the ground breaking ceremony for the accumulation ring (AR) took place.

AR was completed in two years. On November 18, 1983, electron beam was successfully accelerated up to 4.8 GeV in AR. During the period from 1983 to 1986, AR was operated for accelerator developments and calibration of the lead-glass counters used for the colliding experiments in MR.

The first overall operation of MR started on 16th of October, 1986. And on October 24, 1986, electrons were accelerated in MR up to 25.5 GeV (0.4 mA), exceeding the energy maximum (23.5 GeV) obtained in PETRA. On November 15, the first experiment to collide  $e^+$  and  $e^-$  beams at (24+24) GeV was started. The beam current at that time was 1 mA for each beam. After adjusting parameters of accelerator optics and trigger conditions of VENUS detector, the first Bhaba scattering was observed in VENUS detector on November 19, 1986.

Colliding beam experiments started from December 1986, at first at the energy of (24+24) GeV, as shown in Table 2. Numbers in hours show the total operation time and those in parentheses denote the time dedicated to the experiment. In the spring shutdown between February and May of 1987, MR had several large-scaled modifications. One of them was installation of 8 wiggler magnets in the quadrant arcs, which improved the beam injection into the MR substantially. The another largest was replacement of the cathode material of the distributed sputter ion pums (DIP) from aluminum to titanium, which reduced the pressure and lengthened the beam life time.<sup>11)</sup>

The number on the right of the Table 2 corresponds to that of high power (1 ~ 1.2 MW) klystrons installed in the MR. During the summer shutdown period in 1987, all the normal conducting cavities were installed and the klystrons were increased from 20 to 26 in number. This year (1988) the machine is being operated at the energy level of (28+28) GeV. And the total running time at this energy level will be about 1100 hrs.

The Table 3 shows the accelerator parameters attained until now (March, 1988). The value on the right line shows the design goal. In the most recent run, the current in MR could be increased to 13.6 mA from about 8 mA reached so far. In the single beam operation, the maximum current of about 5 mA/bunch has been reached. We observed that one of the reasons why beam current had been limited so low was a synchro-betatron resonance. In the operation started in Jan. 1988, this resonance was carefully avoided by fine adjustment of betatron and synchrotron tunes. Usually MR is first filled with two positron bunches, and then with two electron bunches. Each bunch is stacked with AR beams cycled three times. It takes about 30 minutes to complete the beam injection in MR. In AR, after the operation as the injector to MR, electron beam is stored and accelerated to 5 ~ 6.5 GeV for the synchrotron radiation research in the SRR hall.

#### IV. COLLIDING BEAM OPERATION OF MR

It takes about 2 minutes to accelerate the injected beams to the top energy. The lattice parameters are then changed from those for injection optics to those for low-beta optics. Present performances of the TRISTAN accelerators are summarized in Table 3.

In order to get the luminosity as high as possible, operating parameters of MR were carefully adjusted so that the horizontal emittance and the coupling between the vertical and the horizontal emittances may become as small as possible.<sup>12)</sup> Fine adjustments of the closed orbit were also required to reduce the background on each detector at the colliding points. The highest peak luminosity attained so far is about  $1.4 \times 10^{31} \text{ cm}^{-2}\text{s}^{-1}$  at total beam current of 13.6 mA and the vertical to horizontal emittance ratio of 1.5 %. Integral luminosity was thus improved up to 300 ~ 400 nb<sup>-1</sup>/day.

A typical operation pattern of MR, which was recorded through 24 hours on Feb. 28, 1988, is demonstrated in Fig 4. The stepwise increase of the current corresponds to the beam injection from AR to MR. Colliding beam experiments usually continues for about one hour for each beam fill. Such an procedure gives the highest integral luminosity under the present accelerator condition. The day in Fig. 4 passed rather quietly without any accidental beam loss. Although the ratio of the running time lost by the machine failure is not so large, the colliding beam experiments are occasionally interrupted by total or partial beam loss mainly due to troubles of the RF system.<sup>13)</sup> Interlocks for too large power reflected from cavities, for example, switch off the drive power to the klystron. The deterioration of the vacuum in the

tube which is caused by accidental gas burst also switches off high voltage of the klystron power supply. Both lead to the decrease of total RF power which is necessary to sustain the accelerated beams. With the improvements of the system and the aging effect with time, however, the rate of RF failure is being decreased.

## V. TRISTAN MR RF SYSTEM<sup>14,15)</sup>

In a storage ring, the required RF power increases with the beam energy so rapidly that the available amount of RF power ultimately limits the maximum energy. For example at  $E = 28 \text{ GeV}$   $I = 10 \text{ mA}$ , synchrotron radiation becomes 220 MeV/turn, and klystron power should be above 900 kW/tube, in consideration of the frequency shift (+ 2.5 kHz) to reduce the horizontal emittance, waveguide loss (7 %) and the power redundancy to compensate for a power reduction which may happen due to failure of one to two klystrons.

In the early stage of TRISTAN, there was a severe problem what is called a "klystron crisis". AR operation has been frequently interrupted by damage of klystrons. Due to the close collaboration between KEK and industries, however, klystrons with good qualities have been successfully developed.<sup>16)</sup> Figure 5 shows the klystron E3786 delivered by Toshiba. The maximum output power is about 1.2 MW in CW with efficiency above 65 %. These are the world biggest figures for the tube in this frequency region. In TRISTAN we also use another 1 MW klystron YK1303 delivered from Valvo of Philips group.<sup>17)</sup>

One of the biggest problem about Toshiba klystron was the window failure. Due to the multipactoring, the ceramic window showed abnormal temperature increase above a threshold level. The same phenomena happened in the RF coupler used in the Alternating Periodic Structure (APS) cavities. A special coating procedure of TiN was developed to suppress the multipactoring and these problems were solved. During the whole period of operation of TRISTAN, no ceramic breakage has been encountered in widows both for 1 and 1.2 MW klystrons and for the APS cavities. The optimum thickness of TiN films was found out by a bench test as shown in Fig. 6. Klystron power output goes through a Y shaped circulator and 100 % reflected by a waveguide short. Reflected power is terminated with a water load on the right. Small ceramic samples are exposed to RF field in a quartz vacuum tube which is placed at an antinode position of the WR1500 (R6) waveguide. From a view port just above the center of the quartz tube, we can measure the temperature with an infrared thermometer and investigate multipactoring on the samples directly. Figure 7 shows the distinct difference in the extent of multipactoring between the coated sample and the sample without coating.

In Fig. 8 one set of the high power RF system of MR is shown. The klystron output is connected to a differential type circulator. One klystron feeds its RF power into four RF cavity units about 10 m underground. Several magic tees as well as the newly developed 1 MW circulator are used in the WR1500 (R6) waveguide system to split the power. Figure 9 shows

a cross sectional view of the APS cavity.<sup>18)</sup> The RF coupler for the cavity is a loop type one with a cylindrical alumina ceramic (97 %) also coated with TiN of about 50 Å in thickness. The cavity is made of a low carbon steel (S20C), the inner surface of which is electroplated with 100 µm thick copper in a pyrophosphorous acid bath.<sup>19)</sup>

Hydrogen diffusion to the vacuum through the iron cavity wall was another big problem, which deteriorated the ultimate pressure about an order of magnitude. It is due to the atomic hydrogen produced in a water channel through iron-water reaction process. A commercial anticorrosive for car engine, which was mixed to water by 2 %, depressed this process very much, and this problem has been already settled. Up to now 26 klystrons are feeding RF power to 104 units of 9 cell APS cavities. Shunt impedance is about 22 MΩ/m, that is, total impedance of 6178 MΩ can be attained. It is about 2.7 times larger than that of PETRA (2300 MΩ) and can sustain about 320 MV of accelerating voltage,  $V_c$ .

## VI. UPGRADING PROGRAM OF TRISTAN

### A) SC RF CAVITY<sup>20,21)</sup>

In KEK R&D work on superconducting RF has been carried out for more than 15 years. At the initial stage, however, efforts were mainly concentrated on C-band (~ 6.5 GHz). From 1980 fundamental study on 500 MHz cavity was started by making niobium structures. Beam tests have been done several times by using firstly one 3 cell, secondly one 5 cell and lastly two 5 cell structures in AR as shown in Table 4. The quality factor,  $Q_0$ , of  $1.5 \sim 2 \times 10^9$  for the accelerating field,  $E_{acc}$ , of 5 MV/m has been observed just after the beam test. Another new test is to be done in AR in this March, too. In April 1986, a two year program started to install 32 units of 5 cell superconducting cavities in the Nikko RF section. Two 5-cell units are adjoined and immersed in one helium bath. Details of cavity-cryostat system are shown in Fig. 10. According to this program the first half of 32 units (8 cryostats) will be installed in the summer of 1988, which will increase the beam energy up to (31+31) GeV. Another half (8 cryostats) will be built in by the end of 1989. When the system is completed, the total accelerating voltage is expected to reach as high as 560 MV which will give the beam energy of (33+33) GeV. Production and performance tests of cavities and cryostats are being carried out now. In vertical tests almost all cavities showed  $Q_0$  larger than  $3 \times 10^9$  at low RF level and  $Q_0$  larger than  $2 \times 10^9$  at 5 MV/m. An example of quality factor as a function of accelerating fields is demonstrated in Fig. 11. Even in a horizontal setup, the maximum  $E_{acc}$  of 7 ~ 8 MV/m and  $Q_0$  of  $1.5 \sim 2 \times 10^9$  for  $E_{acc}$  of 6 MV/m have been reached. The liquid helium refrigerator system is also now under construction.<sup>22)</sup> In designing it, we assumed the minimum  $Q$  value of the cavity to be  $1 \times 10^9$  at the target accelerating field of 5 MV/m (See the thick cross in Fig. 11), and obtained an estimated refrigerator cooling power of 6.5 kW at 4.4 K, including heat

leaks and a sufficient safety factor. The refrigerator system for SC cavities is illustrated in Fig. 12. When one replaces the cavities at Oho RF section with SC ones, the upper bound of the beam energy can be extended to approximately (35+35) GeV with the accelerating voltage of about 700 MV.

#### B) SC QUADRUPOLE MAGNET (QCS)<sup>23)</sup>

In order to improve the MR luminosity, we will install superconducting quadrupole magnets (QCS) to realize mini-beta insertion optics. The design is almost fixed as listed up in Table 5. The 4-layer shell type coil of 140 mm in diameter is used. An iron free structure with stainless steel collars is chosen. The designed field gradient is 70 T/m. Three prototypes were constructed in KEK and tested. A field gradient of 80 T/m was reached with very low multipole components. One prototype system is now under construction and will be tested soon. Four systems will be installed in four colliding regions in FY 1989. It is located very close to the collision point in the experimental detector as shown in Fig. 13. The mini-beta optics will give  $\beta_H = 0.8$  m,  $\beta_V = 0.05$  m and will double the luminosity attained with the low-beta optics.

#### C) POLARIZATION

It is well known that electrons (positrons) in the storage ring polarized antiparallel (parallel) to the magnetic field by the spin-flip synchrotron radiation. The polarization build up time  $\tau_{pol}$  varies as

$$\tau_{pol}(s) = 98.66 \frac{[\rho(m)]^3}{[E(\text{GeV})]^5} \times \frac{R}{\rho} \quad ,$$

where  $R$  is the average ring radius. For TRISTAN it amounts to 24 min at 17 GeV and 2 min at 28 GeV. To investigate the weak interaction process, the transverse polarization has to be turned into the longitudinal polarization at the interaction point. This can be accomplished with a system of properly combined horizontal and vertical bends. The maximum polarization attainable for the ideal machine is calculated to be  $8/(5\sqrt{3}) = 0.924$ . In practice, however, depolarizing effects become more and more severe at high energies due to imperfect polarization rotation, closed orbit distortions, beam-beam interactions, and so on, and the polarization may be reduced considerably. A setup to measure the polarization with circularly polarized photon beam of a laser is now in preparation. Spin dependence of the Compton scattering cross-section will be used.

## ACKNOWLEDGEMENT

The author wishes to thank Professor Y. Kimura for his encouragement and careful reading of the manuscript. He is also indebted to Professors S. Ozaki and H. Baba for their encouragements. Many persons who kindly informed him of the latest activities and new results are gratefully acknowledged, too.

## REFERENCES

- 1) S. Ozaki, Proc. 1987 ICFA Seminar on Future Perspectives in High Energy Physics, BNL 1987, 83.
- 2) Y. Kimura and H. Baba, Proc. 6th Symposium Accelerator Science and Technology, Tokyo 1987, 15.
- 3) G. Horikoshi and Y. Kimura, Proc. Particle Accelerator Conference, Washington 1987, KEK Preprint 87-23.
- 4) T. Nishikawa, Proc. 1985 Int. Symp. on Lepton and Photon Interactions at High Energies, Kyoto 1985, 791.
- 5) Y. Kimura, Proc. 13th Int. Conf. on H.E. Accelerators, Novosibirsk 1986, vol.1, 44.
- 6) H. Ishimaru et al., IEEE Trans. Nucl. Sci. NS-30, 2906 (1983).
- 7) A. Kabe et al., Proc. Particle Accelerator Conference, Washington 1987, KEK Preprint 86-119.
- 8) T. Ieiri et al., op. cit., KEK Preprint 87-21.
- 9) S. Takeda et al., IEEE Trans. Nucl. Sci. NS-32, 2062 (1985).
- 10) S. Kurokawa, Proc. Europhysics Conference on Control Systems for Experimental Physics, Villars 1987, KEK Preprint 87-115.
- 11) H. Ishimaru et al., Proc. 6th Symposium Accelerator Science and Technology, Tokyo 1987, 138.
- 12) K. Satoh et al., op. cit., 18.
- 13) M. Ono et al., op. cit., 129.
- 14) K. Akai et al., Proc. 13th Int. Conf. on H.E. Accelerators, Novosibirsk 1986, vol.2, 303.
- 15) E. Ezura et al., Proc. Particle Accelerator Conference, Washington, 1987, KEK Preprint 87-33.
- 16) S. Isagawa et al., op. cit., KEK Preprint 87-7.
- 17) W. Schmidt, Proc. 13th Int. Conf. on H.E. Accelerators, Novosibirsk 1986, vol.2, 319.
- 18) T. Nishikawa et al., Rev. Sci. Instr. 37, 652 (1966).
- 19) T. Higo et al., Proc. Particle Accelerator Conference, Washington 1987, KEK Preprint 87-4.
- 20) T. Furuya et al., 3rd Workshop of RF Superconductivity, Argonne 1987, 95.
- 21) S. Noguchi et al., op. cit., 605.
- 22) K. Hara et al., Advanced Cryogenic Engineering, 615 (1987).
- 23) K. Tsuchiya et al., Advances in Cryogenic Engineering, vol.31, 173 (1986).

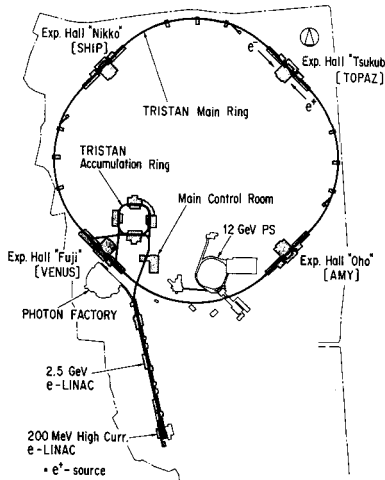


Fig. 1 Layout of TRISTAN.

Table 1 Parameters of the TRISTAN AR and MR.

|                                    | AR                | MR          |
|------------------------------------|-------------------|-------------|
| Circumference                      | 377 m             | 3018 m      |
| Average radius of curved section   | 47.7 m            | 346.7 m     |
| Bending radius                     | 23.2 m            | 246.5 m     |
| Long straight sections             | 2 x (19.5m+19.1m) | 4 x 194.4 m |
| Total length of RF cavity sections | 30 m              | 400 m       |
| RF frequency                       | 508.6 MHz         | 508.6 MHz   |
| Injection energy                   | 2.5 GeV           | 7.4 ~ 8 GeV |
| Maximum energy                     | 7.4 ~ 8 GeV       | 28 GeV      |

Table 2 Colliding beam experiments in TRISTAN.

| Period       | Beam Energy                   | Operation time | # of Klystron |
|--------------|-------------------------------|----------------|---------------|
| 1986 DEC     | (24+24)GeV                    | 182(104)h      | 16            |
| 1987 JAN-FEB | (25+25)GeV                    | 596(281)h      | —             |
| MAY-JUN      | (25+25)GeV                    | 737(368)h      | 20            |
| JUN-JUL      | (26+26)GeV                    | 707(530)h      | —             |
| 1987 OCT-DEC | (27.5+27.5)GeV                | 1310(724)h     | 26            |
| 1988 JAN-MAR | (28+28)GeV                    | 1170(650)h     | —             |
| 1988 FALL    | Energy up to 30 ~ 33 GeV      | —              | 30            |
|              | SC Cavity in Nikko RF section |                |               |

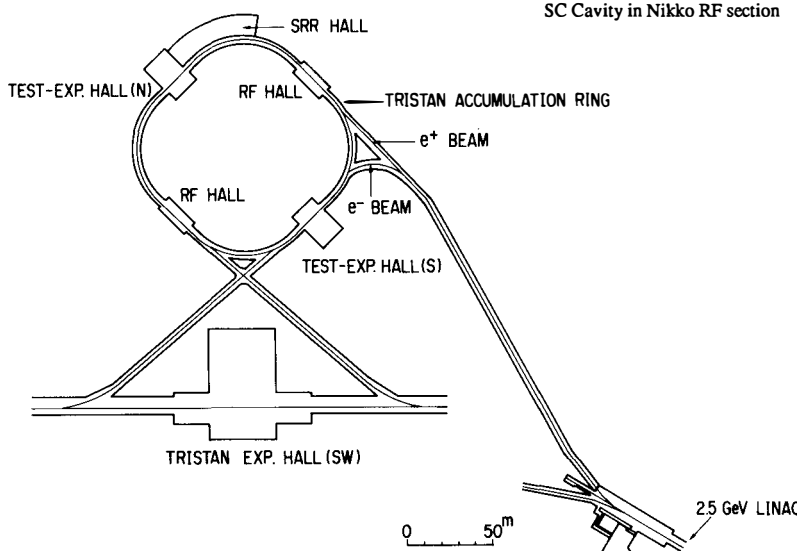


Fig. 2 Accumulation ring and beam transport lines.

Table 3 Accomplished accelerator parameters, March 1988.

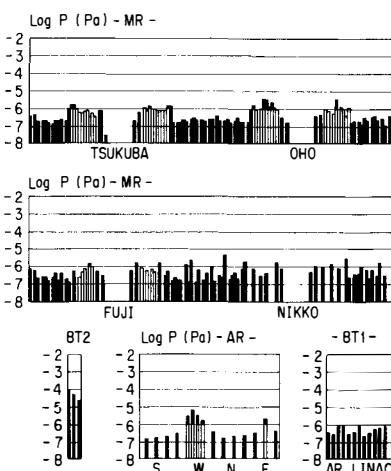


Fig. 3 Pressure distribution in TRISTAN AR, BT and MR.

|                      | INJECTOR LINAC                                      | ACHIEVED  | DESIGN GOAL |
|----------------------|---|---|-------------|
| E BEAM               | : 2.5 GeV   | 2.5 GeV   |             |
| I BEAM               | : $e^- > 50$ mA                                     | 50 mA   | 50 mA       |
| REP. RATE            | : 25 Hz   | 50 Hz   | 50 Hz       |
| BEAM WIDTH           | : 1 ns (HWHM)                                       | 1 ns  | 1 ns        |
| ACCUMULATION RING    |   |   |             |
| E BEAM               | : 7.5 GeV   | 8 GeV   |             |
| I BEAM               | : 20 mA typical                                     | 20 - 30 mA                                      |             |
| MAIN RING            |   |   |             |
| E BEAM               | : 28 GeV  | 30 GeV  |             |
| I BEAM               | : 13.6 mA total (4 bunch)                           | 15 mA   |             |
|                      | 4.8 mA/bunch (1 beam)                               |   |             |
| BEAM LIFE            | : 2 - 3 h   | 4 - 5 h   |             |
| INJ. EFF.            | : 50 - 80 %   | 80 %  |             |
| # OF IR              | : 4   | 4   |             |
| # OF BUNCH           | : 2 for $e^-$ , 2 for $e^+$                         | 2 + 2   |             |
| HORIZ. TUNE          | : 36.609  |   |             |
| VERT. TUNE           | : 38.680  |   |             |
| BEAM-BEAM TUNE SHIFT |   |   |             |
| HORIZ.               | : 0.02 at $I = 12$ mA                               | 0.03  |             |
| VERT.                | : 0.03 at $I = 12$ mA                               | 0.03  |             |
| $\beta^*H$           | : 1.8 - 2 m   | 1.6 m   |             |
| $\beta^*V$           | : 0.1 m   | 0.1 m   |             |
| V-H EMIT. RATIO      | : 1 ~ 2 %   |   |             |
| PEAK LUM.            | : $1.4 \times 10^{31} \text{ cm}^{-2}\text{s}^{-1}$ | $1 \times 10^{31} \text{ cm}^{-2}\text{s}^{-1}$ |             |
|                      | @ 13.6 mA   |   |             |
| LUM. INTEG.          | : 300 - 400 nb <sup>-1</sup> /day                   |   |             |

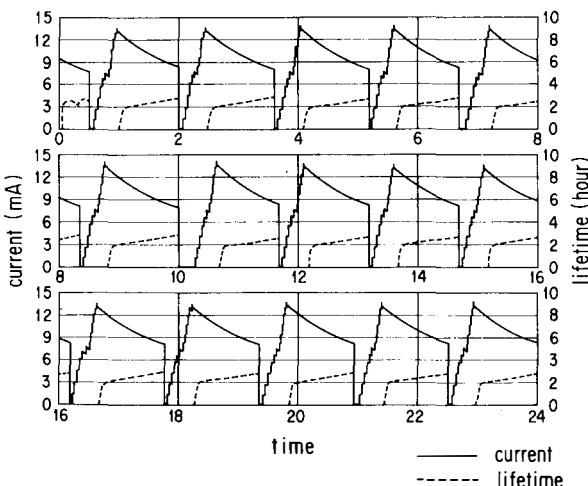


Fig. 4 One-day colliding beam operation of TRISTAN.

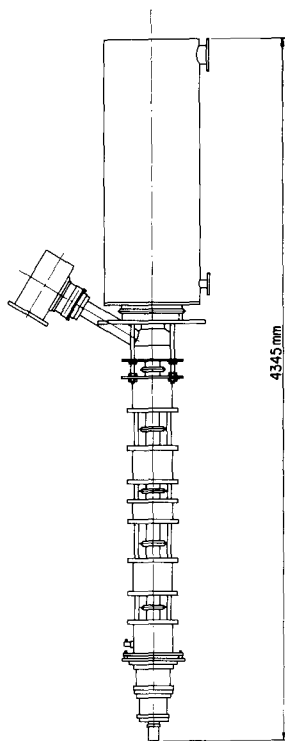


Fig. 5 1.2 MW CW klystron, E3786,  
developed for TRISTAN.

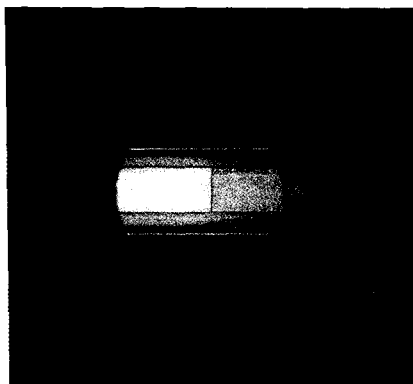


Fig. 7 Suppression of multipacting  
by TiN coating.

Sample on the left:  
 $\text{Al}_2\text{O}_3$  without coating  
Sample on the right:  
 $\text{Al}_2\text{O}_3$  with 120 Å TiN

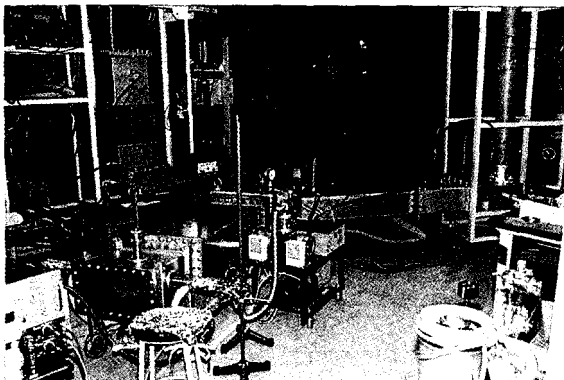


Fig. 6 Test bench for studying multipacting phenomena.

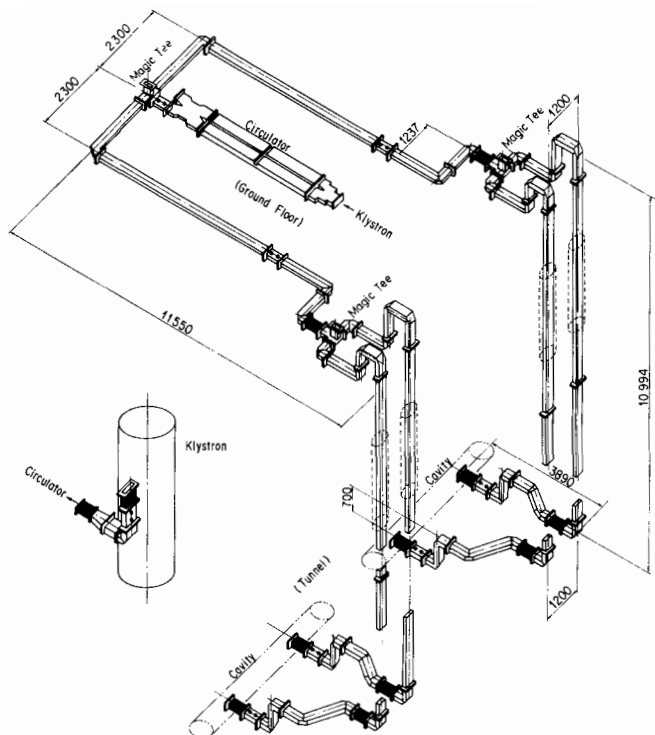


Fig. 8 High power R F system (1 klystron unit).

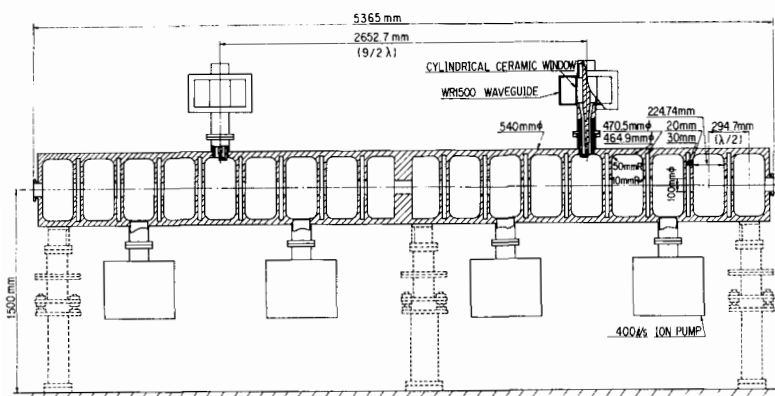


Fig. 9 Alternating Periodic Structure (APS) cavity.

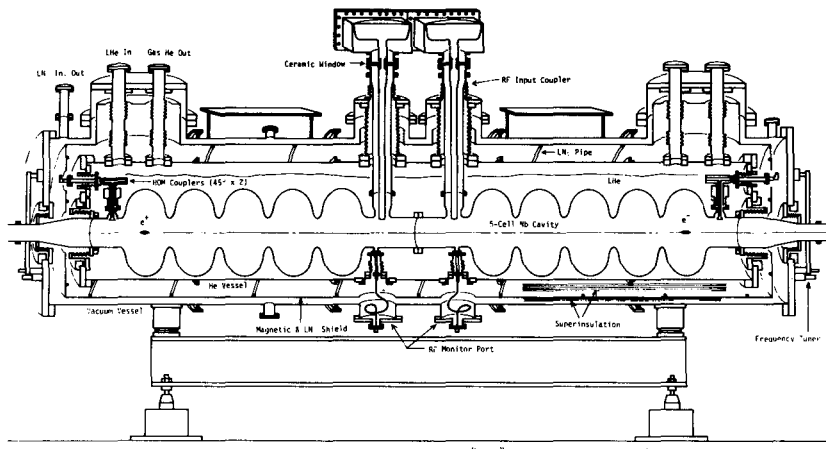


Fig. 10 Superconducting cavity for TRISTAN MR.

Table 4 Beam tests of SC cavity in AR.

| Date   | E(GeV)        | I(mA) | Eacc (MV/m)   | RF power to beam (kW) |
|--|---------------|-------|---------------|-----------------------|
| 1984 MAY 1st acceleration in AR (1 x 3 cell) |               |       |               |                       |
|  | 4.6           | 1.6   | 3.5           | 3                     |
| JUL  | 5.0 (SC)      | 1.0   |               |                       |
|  | 6.5 (SC+NC)   | 0.4   | 4.3           |                       |
| 1986 FEB 2nd test in AR (1 x 5 cell)         |               |       |               |                       |
|  | 2.5           | 28    | 3.0 (beam)    | 26                    |
|  | 4.8           | 12.8  | 4.5 (no beam) |                       |
| 1987 OCT 3rd test in AR (2 x 5 cell)         |               |       |               |                       |
| - NOV  | 2.5 (1 x SC)  | 50    |               |                       |
|  | 5.5 ( " )     | 20    |               | 68.2                  |
|  | 6.5 (2 x SC)  | 15    | 5.3           | 99.6                  |
|  | 7.7 (SC + NC) | 6     |               |                       |

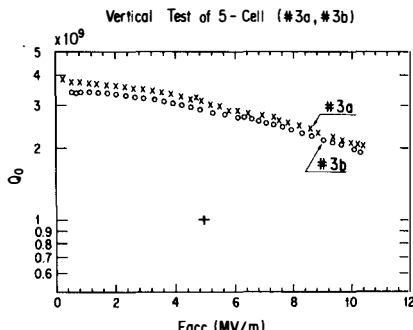


Fig. 11 Measured Q-values of one pair of superconducting five-cell cavities for MR, as a function of the accelerating field.

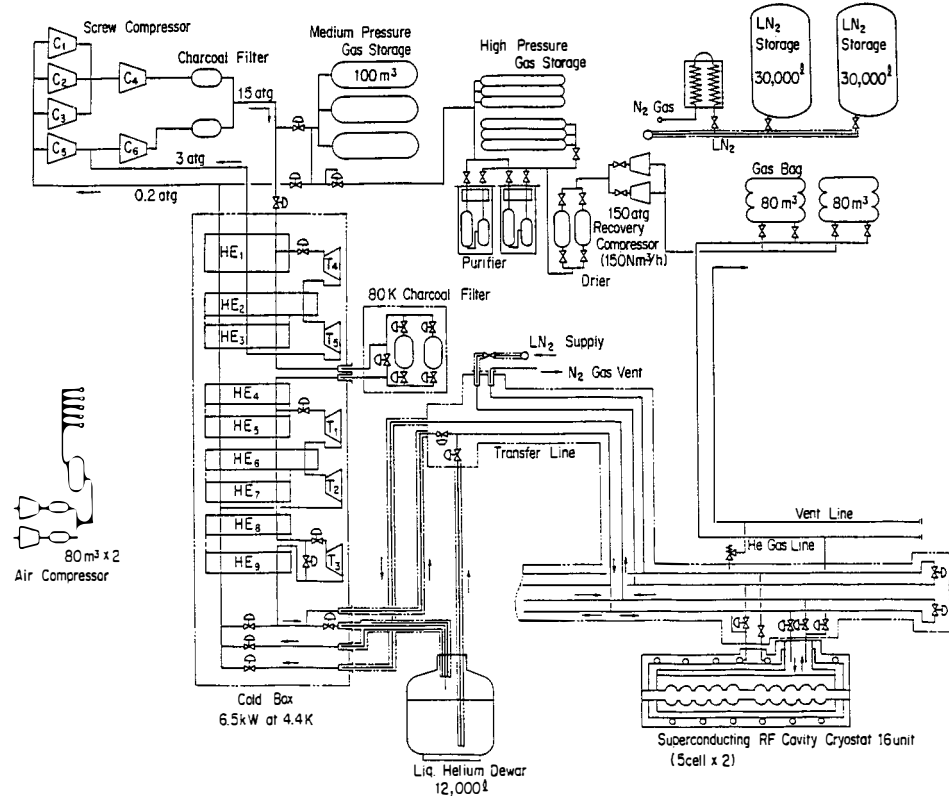


Fig. 12 Flow diagram of the helium refrigerator system for the superconducting RF cavity.

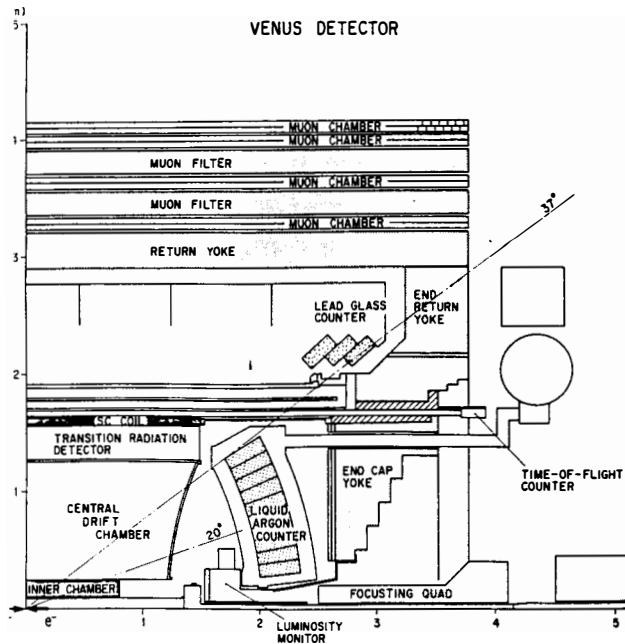


Fig. 13 QCS in the VENUS DETECTOR.

Table 5 Parameters of insertion quadrupole (QCS).

|                           |                    |
|---------------------------|--------------------|
| Field gradient            | 70 T/m             |
| Current                   | 3400 A             |
| Magnetic length           | 1100 mm            |
| Coil (4-layer shell type) |                    |
| inner diameter            | 140 mm             |
| outer diameter            | 217 mm             |
| Field uniformity          |                    |
| $\Delta G/G$              | $1 \times 10^{-3}$ |
| Stored energy             | 341 kJ             |
| Bursting force            | 94 ton/m           |